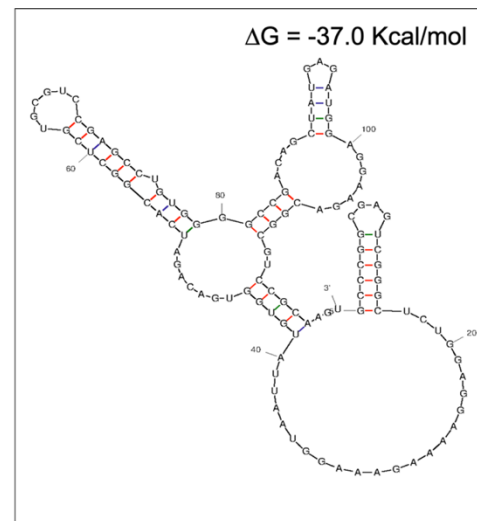
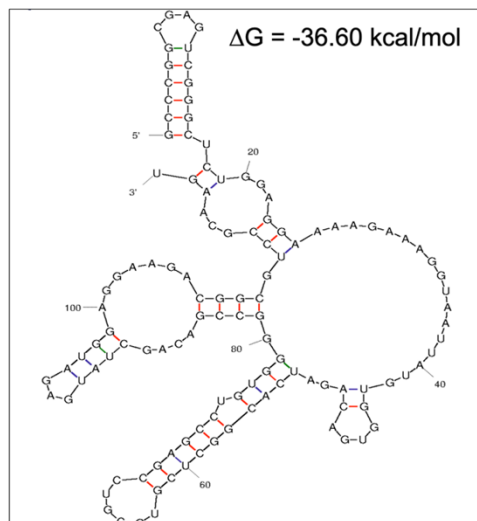
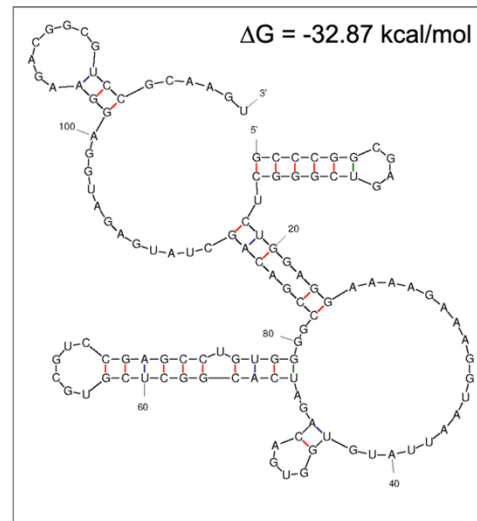
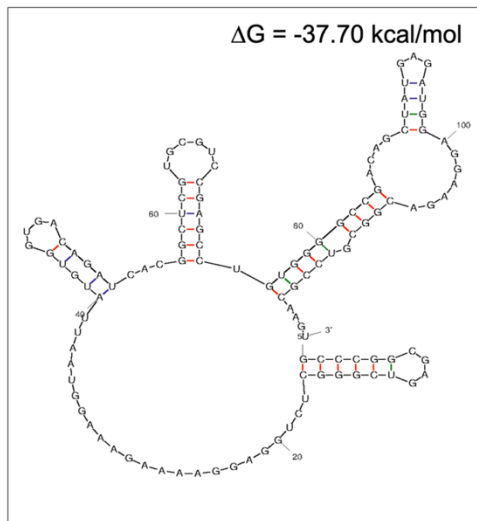


Supplementary Figure 1

EGFRVIII target amplicon

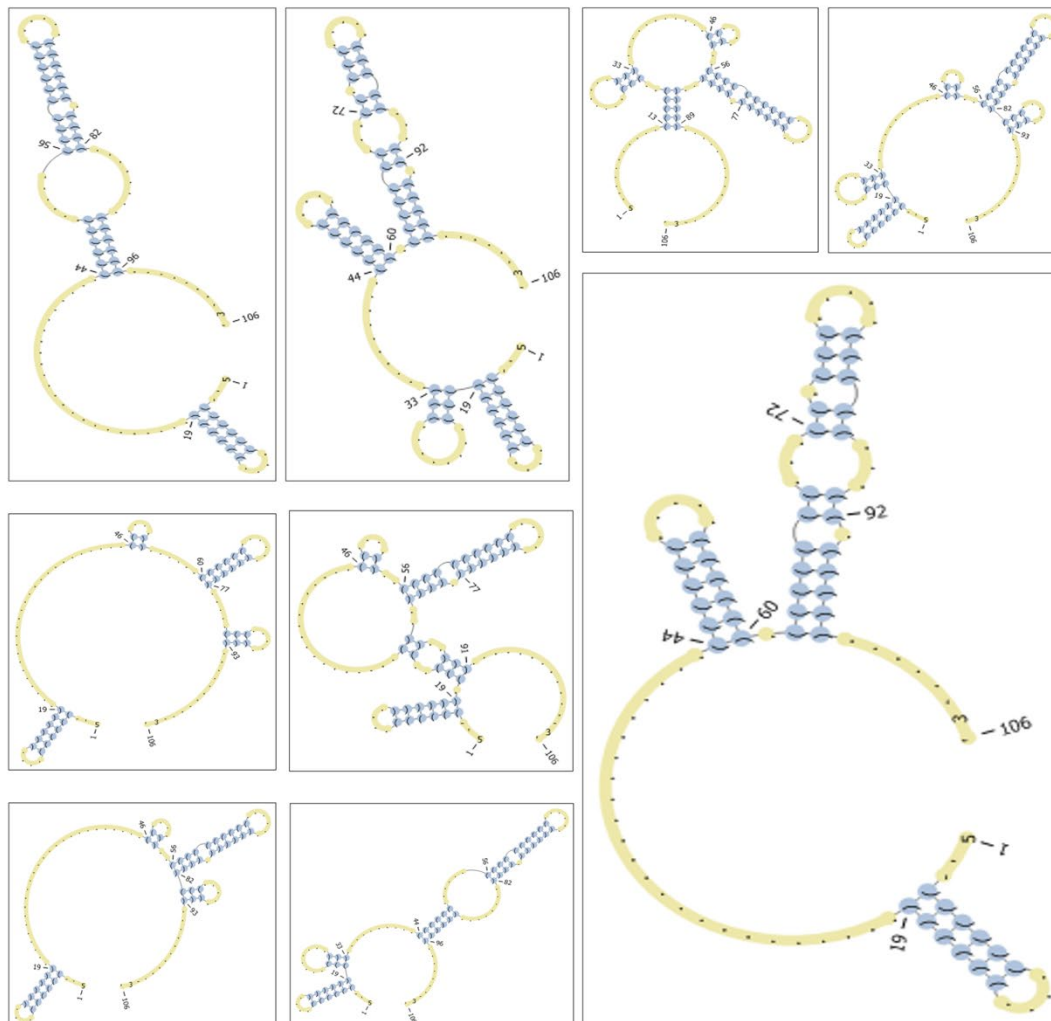
a.



Supplementary Figure 1 (continued)

EGFRvIII target amplicon

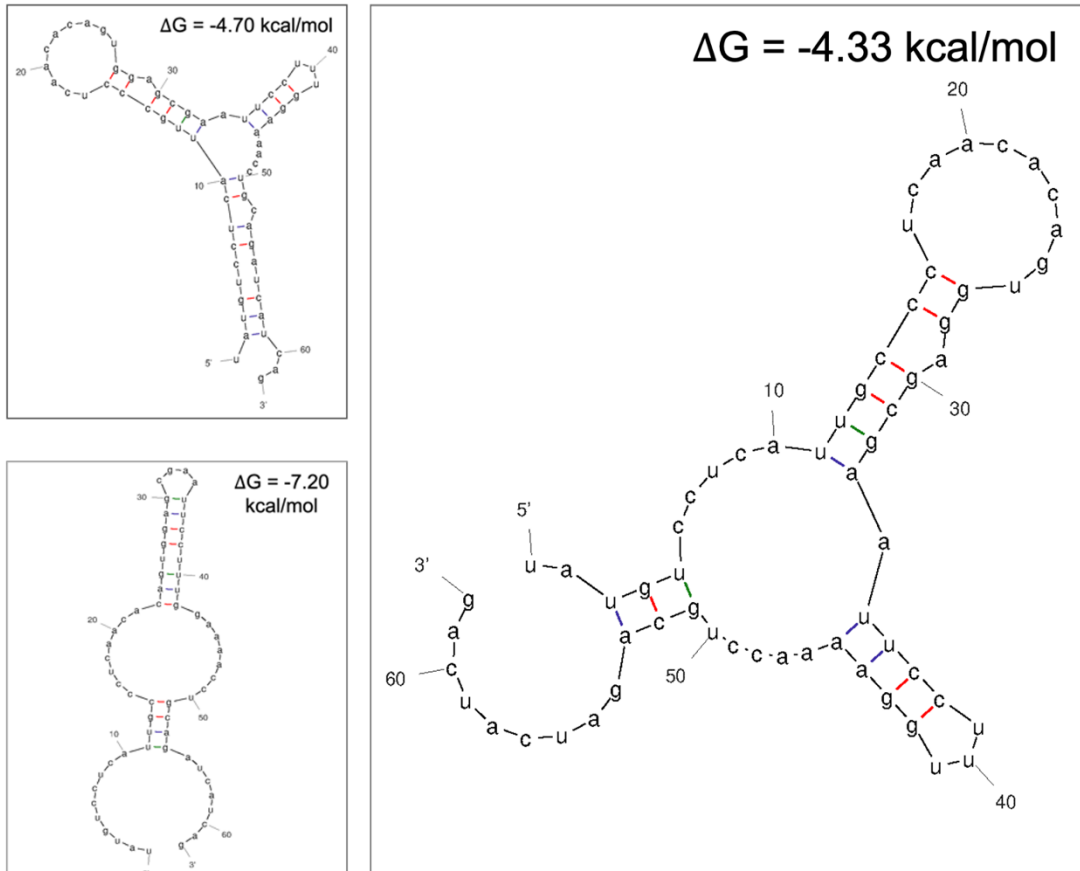
b.



Supplementary Figure 1 (continued)

EGFRwt target amplicon

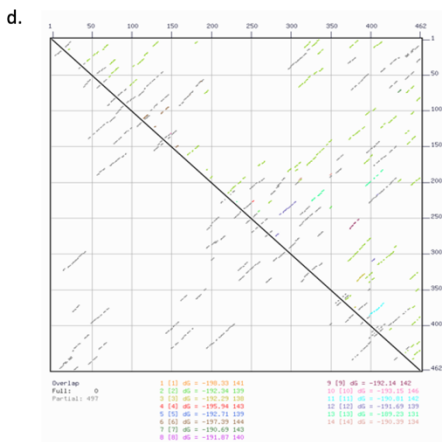
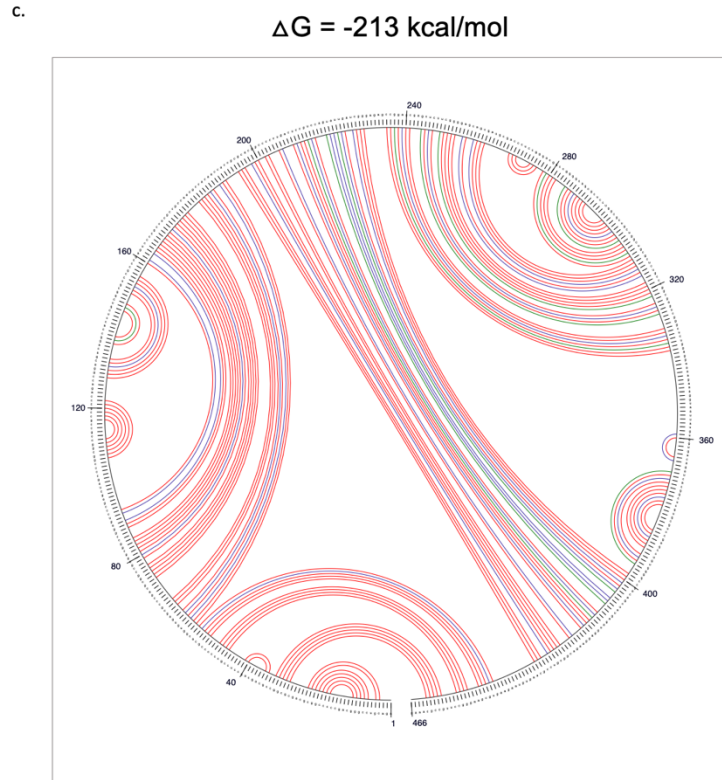
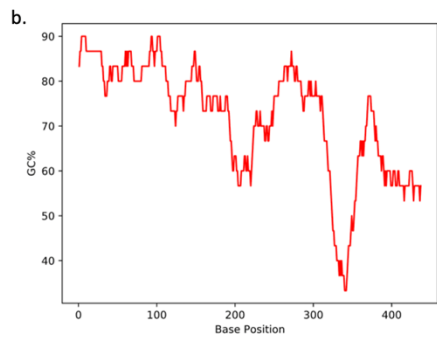
c.



Supplementary Figure 1: Secondary Structure prediction in target amplicon of EGFRvIII and EGFR wt using Mfold algorithm. (a) Four distinct secondary structures in target amplicon (96 bp) of EGFRvIII with minimum free energy (ΔG) in the range of (-32.87 to -37.70) kcal/mol. **(b)** Depiction of nine potential pseudoknots in target amplicon of EGFRvIII as predicted by algorithm. **(c)** Three possible secondary structures predicted in EGFR wt target amplicon (62 bp) with ΔG in the range of (-4.33 to -7.20) kcal/mol.

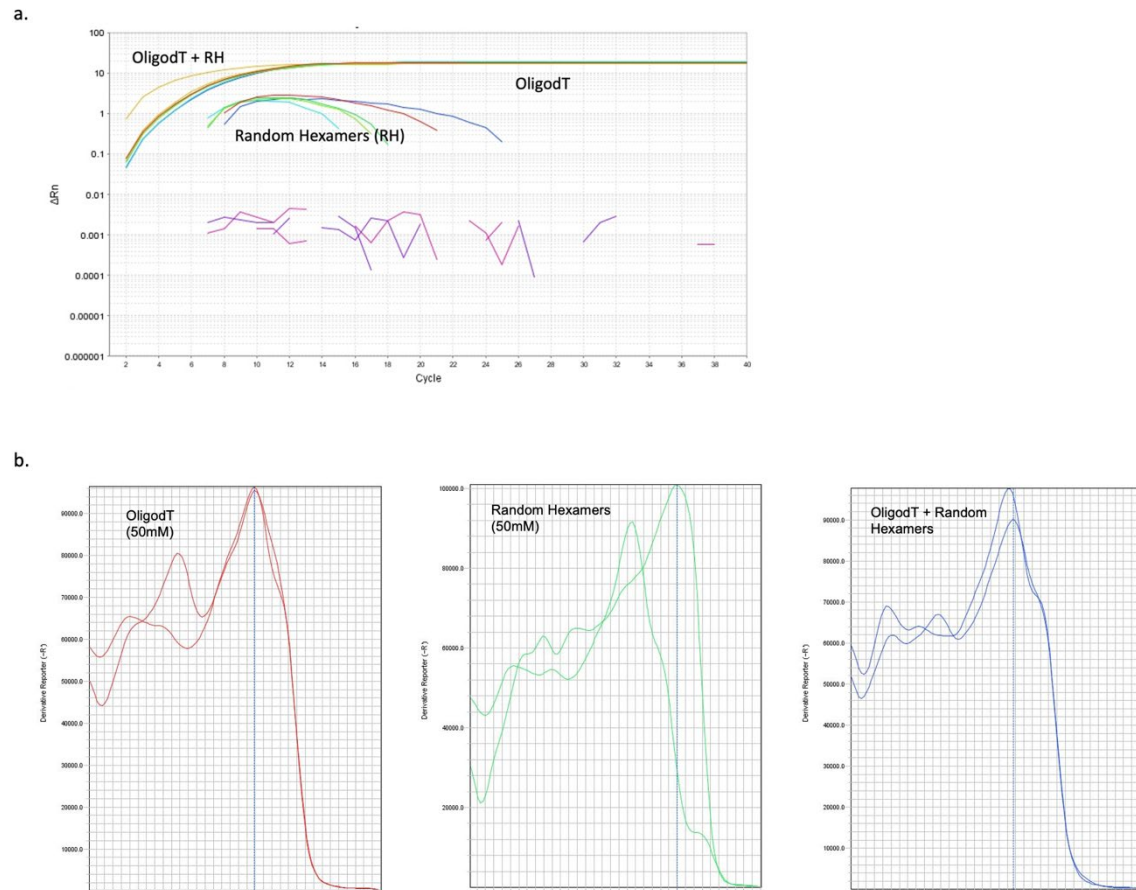
Supplementary Figure 2

a. AGACGTCCGGGCAGCCCCGGCGCAGCGCGCCGAGCAGCCTCCGCCCCCGCACGGTGTGAGCGC
 CCGACGCGGCCGAGGCGGCCGAGTCCCGAGCTAGCCCGGCGGCCGCGCCGCCAGACCGGACGA
 CAGGCCACCTCGTCGGCGTCCGCCGAGTCCCGCCTCGCCGCAACGCCACAACCACCGCGCACGGC
 CCCTGACTCCGTCCAGTATTGATCGGGAGAGCCGGAGCGAGCTCTTCGGGGAGCAGCGATGCGACCTC
 CGGGACGGCCGGGCAGCGTCCCTGGCGTGCTGGCTGCGCTCTGCCCGCGAGTCCGGCTCTGGAG
 GAAAAGAAAG//GTAATTATGTGGTGACAGATCACGGCTCGTGGTCCGAGGCTGTGGGCGCG
 ACAGTATGAGATGGAGGAAGACGGCTCCGAAGTGTAAAGATGGGAAGGCTTSCCGCAAAG



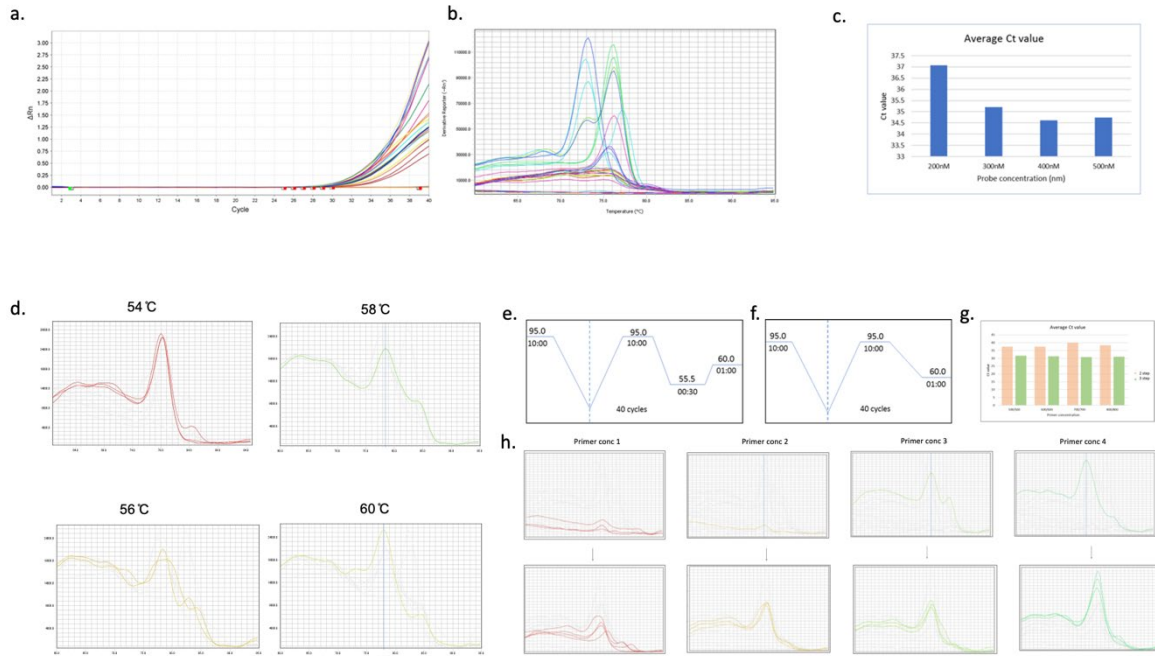
Supplementary Figure 2: Analysis of nucleotide sequence (467 bp) unique to EGFRvIII at exon1:exon8 junction site (a) Nucleotide sequence of exons 1:8 fusion where EGFRvIII occurs, highlighting GC, CG and G repeats. **(b)** Graphical representation of the GC content (percentage) in the nucleotide sequence of exon1:exon8 with the calculation based on window size of 30 bases. **(c)** Circle graph obtained from secondary structure prediction analysis illustrating the individual base pair interactions in 20 predicted foldings. Each color represents a distinct base pair interaction. The ΔG indicating the thermal stability of the predicted foldings is -213 kcal/mol. **(d)** Energy dot plot of the computed foldings, with different dots representing the superposition and relative thermal stability of all possible foldings.

Supplementary Figure 3



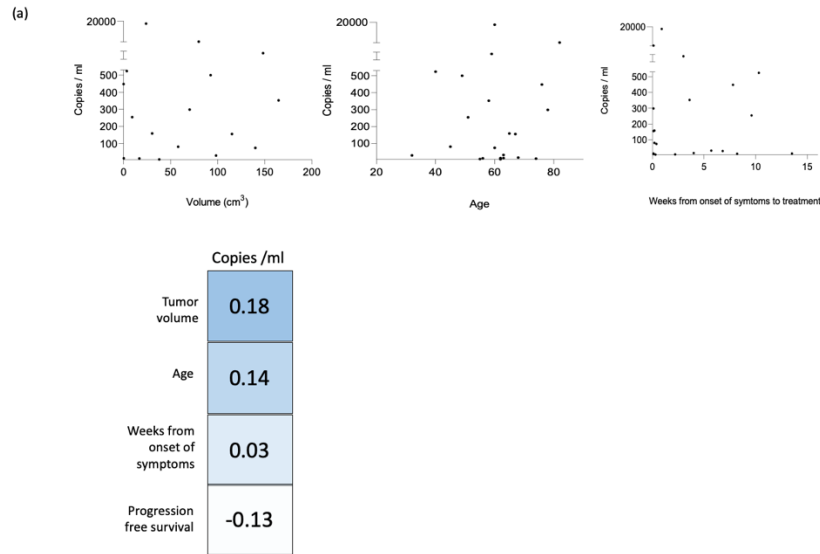
Supplementary Figure 3: Summary of optimization measures. (a) Amplification plot demonstrating the effect of using oligodT and Random hexamers in different combinations during reverse transcription on resulting Ct value in qPCR. **(b)** Melt curve plots illustrating the maximum peak and T_m value of the qPCR product in the three different reverse transcription conditions.

Supplementary Figure 4



Supplementary Figure 4: Summary of qPCR optimization measures. Amplification plot (a) and melt curve plot (b) obtained by testing different concentrations of forward and reverse primers. Amplification plot demonstrating the Cycle threshold (Ct) values obtained at different probe concentrations (c). Annealing temperature gradient (54-60) $^{\circ}$ C assessment to determine the peak of target product and prevalence of non-specific products as shown on melt curve plots (d). Schematic depicting the three step (e) and two step (f) qPCR cycling conditions. Bar graph (g) demonstrating the lowering of Ct value at four different forward/reverse primer concentrations with the use of three step (green bar) vs two step (orange) cycling conditions. Melt curve plots (h) from two step (top panel) and three step (bottom panel) cycling conditions at four different primer concentrations comparing the maximum peak of the target product.

Supplementary Figure 5



(b)

Patient ID	T1	T2	Longitudinal sample
Wt2	0	0	N/A
Wt5	0	0	N/A
P20	5.2	3.1	8.6
Wt8	0	0	N/A
P16	4.7	3.3	3.5
P10	6.9	4.2	9.1
Wt3	0	0	N/A

Supplementary Figure 5: Reproducibility and intratumoral heterogeneity

(a) Linear regression (top) and correlation matrix (bottom) between copies/ml and clinical parameters. (b) Detection of EGFRvIII mutant levels in plasma derived EV RNA, in a group of EGFRvIII patients (P10, P16, P20) and controls (Wt3, Wt5, Wt8) at two different time points, T1 and T2. The copies of EGFRvIII are normalized to GAPDH run in the same well. Third column represents EGFRvIII copies (normalized to GAPDH) in longitudinal samples.

Supplementary Table 3

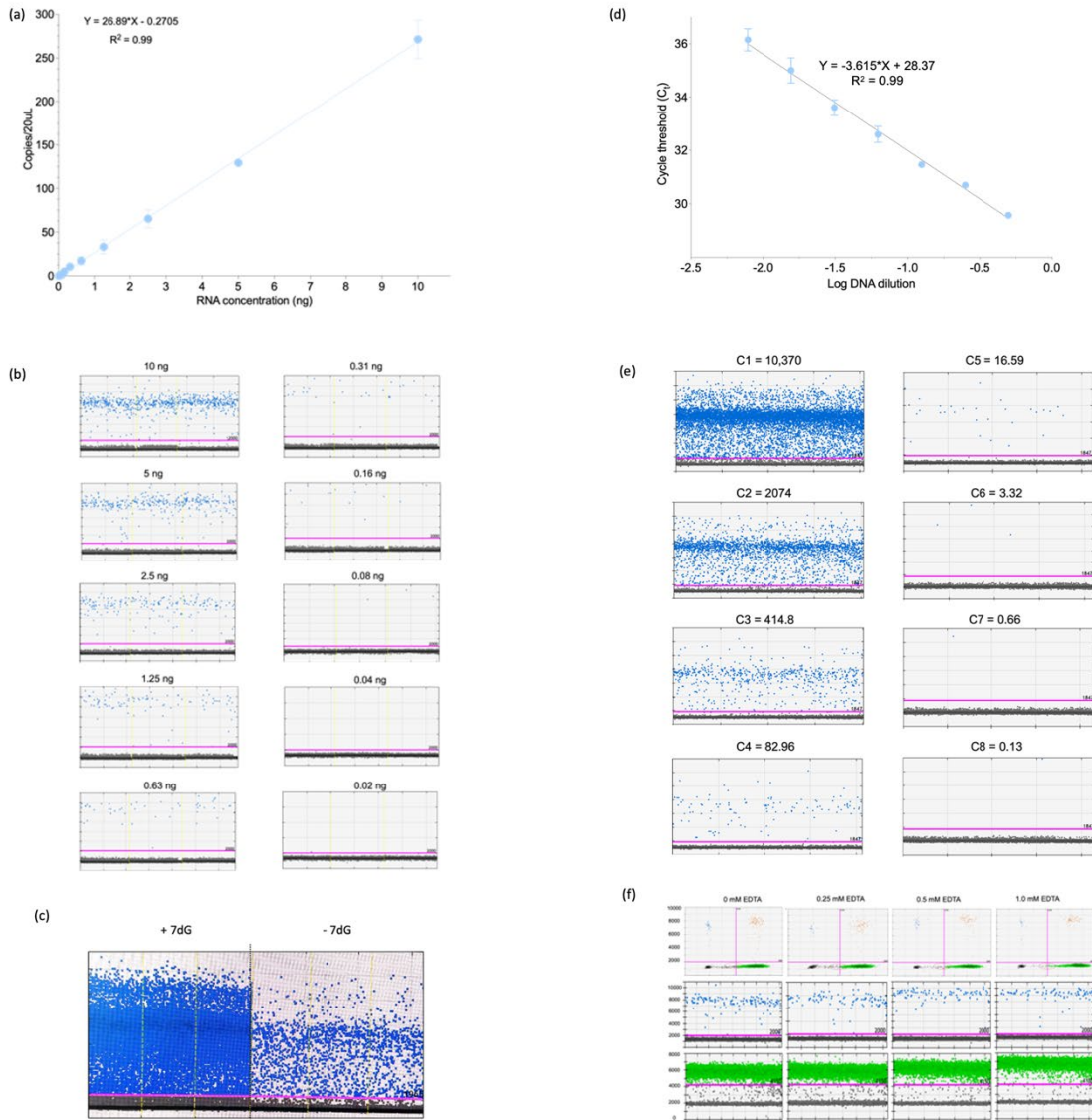
Cohort 2

Study ID	Ct rep 1	Ct rep 2	Avg_GAPDH	Ct rep 1	Ct rep 2	Avg_EGFPwt	Ct rep 1	Ct rep 2	Avg_EGFPwt	Norm_GAPDH	Norm_EGFPwt	Norm_EGFPwt
MGH-19012	18.3007984	18.2145844	18.25769138	25.4956028	25.08634567	25.29097748	28.7928333	28.8824825	28.8376079	0.80724301	24.48373318	28.03041649
MGH-19006	18.2436118	17.7154045	17.97951126	22.6824047	22.69255638	22.68748093	35.62703	36.73383	36.19042946	0.529064178	22.15841675	35.65136528
BC-17014	17.4554996	18.2439938	17.8497467	16.46021843	16.56148529	16.51085186	35.34437561	32.78369904	34.06433752	0.39929922	16.1155224	33.6647277
MGH-18056	19.1898201	19.122864	19.1563421	18.9460113	19.0589161	19.0024637	21.43121719	21.73722504	21.59422112	1.705895017	17.29656868	19.8883261
MGH-19108	18.0961285	18.2877941	18.19198129	16.6451599	16.93544579	16.78998089	30.032938	30.70248604	30.38771202	0.741514206	16.04846668	29.62619781
MGH-21017	17.6818218	17.6644592	17.67314053	16.83738327	16.50945473	16.673419	30.3235281	27.02560425	28.67447853	0.228933443	16.45072556	28.45178509
MGH-20035	18.2074375	17.3450603	17.78248983	20.22495842	19.74502563	19.98499203	23.72048	23.76638	23.74342918	0.325801849	19.65919018	23.41782273
MGH-20084	18.5624428	17.7538863	18.15816402	24.99819183	25.07386589	25.03602886	34.96829987	35.30978775	35.13904381	0.707716942	24.32831192	34.3132887
MGH-18134	18.2077579	18.4575672	18.33266258	19.78232384	20.00311279	19.89271832	31.90046883	29.71730042	30.80888462	0.8822155	19.0100282	29.92666912
BC-17017	18.1289112	17.8028183	17.96486473	19.69542684	19.0052589	19.37797642	25.68888392	25.82143402	25.75520897	0.514417648	18.86355877	25.24079132
MGH-18126	18.674136	19.7245007	18.29931831	22.41388647	21.30988884	21.86189385	24.10434151	23.56221771	23.83327961	0.848871231	21.0130242	22.98400838
MGH-18087	18.128294	17.8565865	17.99246022	17.4209919	17.51852226	17.46975708	35.48660492	32.58485712	34.04078102	0.541993141	16.92776394	33.49878788
MGH-20101	17.5928908	17.4765072	17.53454399	21.78619911	21.10041237	21.43330574	25.35233498	25.6563225	25.50898361	0.08409609	21.34920883	25.4248867
MGH-20082	17.5004639	17.4350948	17.48777439	23.95437995	23.94470978	23.94909286	31.50045967	31.62404251	31.56225109	0.017327309	23.93176556	31.54492378
MGH-19149	17.4770203	17.4238739	17.46044708	25.36227228	24.76921654	25.0657444	40	40	40	0	25.0657444	40
BC-18032	17.5515838	17.6874275	17.61934566	22.28536415	22.23291588	22.25914001	22.32438278	22.00032616	22.16235447	0.16889562	22.09024143	21.99345589
MGH-19093	17.8883724	18.3876057	18.13798904	30.82841	30.81092	30.818665	40	40	40	0.687541962	30.1123504	39.1245804
MGH-19149	17.9953871	17.7803165	17.89034176	22.44480061	21.9545933	22.20151997	40	40	40	0.439894676	21.7612529	39.56010532
BC-18037	18.0925293	17.6841471	17.8933382	21.95669365	22.41148758	22.18409081	27.92067528	27.77781868	27.84924688	0.442891121	21.74119949	27.40635086
MGH-18081	17.743214	17.652309	17.64771652	16.42099119	16.64805603	16.53452396	31.90290642	33.7375412	32.82022381	0.19728944	16.33725452	32.62295437

Cohort 3

Patent ID	Ct rep 1	Ct rep 2	Avg_gapdh	Ct rep 1	Ct rep 2	Avg_egt	Ct rep 1	Ct rep 2	Avg_EGFPwt	Norm_gapdh	Norm_egt	Norm_EGFPwt
MGH-20104	27.50389862	27.72080231	27.61235046	30.18013763	30.34205055	30.26109409	40	40	40	7.6563797	22.80471439	32.3436203
MGH-20192	23.25525566	24.0925707	23.87391882	25.15888405	24.94959831	25.05424118	38.36100388	37.01246282	36.88673325	3.717946053	21.33629513	32.96878719
MGH-20112	25.95660973	25.6935988	25.80798435	27.6222694	27.9166832	27.78446007	40	40	40	5.852013588	21.93244648	34.14786841
MGH-21087	24.6199529	25.6025334	25.10974312	28.36639977	28.60464287	28.48552132	36.58282303	37.4393959	37.01610947	5.153772354	23.33174896	31.86233711
MGH-20152	24.40704918	24.97627721	24.69266319	20.07348633	19.44069888	19.75704765	34.93694305	34.45499039	34.89596672	4.736692429	15.02035522	29.95927429
MGH-21029	19.749860736	20.16213417	19.95597076	21.94208145	21.76098287	21.85148716	31.34784807	32.48620605	31.91707706	0	21.85148716	31.91707706
MGH-21053	27.92509651	27.8609127	27.94300461	28.7177906	26.40461731	26.56120396	33.48728012	34.1177597	33.80751991	7.987033844	18.57417011	25.82048607
MGH-21038	24.78341866	24.4810276	24.6322313	27.94438171	28.32129288	28.1328373	36.57641602	37.40880203	36.99209092	4.676252365	23.45658493	32.1635666
MGH-21042	27.9183882	27.5788689	27.83486176	29.03850604	28.60367393	28.81790909	40	40	40	8.787890991	20.9382	32.1210961
MGH-21017	20.97009277	20.61478135	20.78242706	18.9414463	19.12094116	19.03119373	32.08821432	32.68430328	32.3987588	0.836466299	18.19473743	27.83802223
MGH-21046	22.45641899	22.2765873	22.36748986	28.46891504	28.19516845	28.33204269	34.95549390	34.93353653	34.94451523	2.411518097	25.9205246	32.53299713
MGH-21056	23.96917152	24.82483292	24.39700222	24.67865143	24.5433445	24.58099796	34.8964022	33.88217377	34.38435099	4.441031458	20.11998651	29.92332554
MGH-20086	24.62409621	24.44667825	24.53537273	22.82577705	22.75073242	22.82002081	33.97887421	33.98954201	33.98954201	4.57940197	18.17133045	29.41014004
MGH-20084	25.42221069	25.41974258	25.42097664	28.03621483	28.40188026	28.21904755	37.81202698	37.87554932	37.84378815	5.465005875	22.75404167	32.37878227
MGH-20100	28.87053871	25.7077198	25.78912926	27.37074471	27.69473839	27.5274155	34.58914902	34.27068903	34.41990852	5.833158493	21.69958305	28.58675003
MGH-20112	29.91491699	29.56849615	29.74220697	31.8421463	32.36932755	32.15573692	40	40	40	9.786235809	22.36950111	30.21376419
MGH-21058	24.41893196	24.28207207	24.30500201	23.77348954	24.12952814	23.95151234	31.32873836	31.91280746	31.619797291	4.38453125	19.55698109	27.22524166

Supplementary Figure 6



Supplementary Figure 6: Assessment of assay efficiency and linearity

EGFRvIII cDNA reverse transcribed from serially diluted tumor tissue RNA was amplified using (a) ddPCR, and (d) qPCR. (a) Linear Regression graph depicting the EGFRvIII copies detected via ddPCR plotted against the RNA input. Regression analysis reported $R^2 = 0.99$. (b) ddPCR 1D plots demonstrating the mutant signal generated at each RNA concentration. (d) qPCR standard curve demonstrating Cycle threshold (C_t) values plotted against the log RNA input. Linear regression analysis reported $R^2 = 0.99$. (c) ddPCR 1D plots depicting the mutant signal generated when EGFRvIII synthetic RNA is reverse transcribed into cDNA with (+) and without (-) 7dG followed by ddPCR amplification. (e) ddPCR 1D plots demonstrating the mutant signal generated when cDNA from serially diluted EGFRvIII synthetic RNA was amplified using ddPCR. C number corresponds to the data point and the EGFRvIII copy number input in each RT condition. (f) ddPCR 2D plots

(top row) and 1D plots depicting cluster density, tightness, and separation of mutant events (blue) and GAPDH events (green) at different concentrations of EDTA versus no EDTA addition to ddPCR.